Approximating the Integral Fréchet Distance

Anil Maheshwari[1], Jörg-Rüdiger Sack[2], and Christian Scheffer[3]

1 **School of Computer Science, Carleton University, Ottawa, Canada**
anil@scs.carleton.ca

2 **School of Computer Science, Carleton University, Ottawa, Canada**
sack@scs.carleton.ca

3 **Department of Computer Science, Braunschweig University of Technology, Braunschweig, Germany**
scheffer@ibr.cs.tu-bs.de

Abstract

We present a pseudo-polynomial time $(1+\varepsilon)$-approximation algorithm for computing the integral and average Fréchet distance between two given polygonal curves T_1 and T_2. The running time is in $\mathcal{O}(\zeta^4 n^4/\varepsilon^2)$ where n is the complexity of T_1 and T_2 and ζ is the maximal ratio of the lengths of any pair of segments from T_1 and T_2.

Furthermore, we give relations between weighted shortest paths inside a single parameter cell C and the monotone free space axis of C. As a result we present a simple construction of weighted shortest paths inside a parameter cell. Additionally, such a shortest path provides an optimal solution for the partial Fréchet similarity of segments for all leash lengths. These two aspects are related to each other and are of independent interest.

1998 ACM Subject Classification F.2 Analysis of Algorithms and Problem Complexity, I.3.5 Computational Geometry and Object Modeling

Keywords and phrases Fréchet distance, partial Fréchet similarity, curve matching

Digital Object Identifier 10.4230/LIPIcs.SWAT.2016.26

1 Introduction

Measuring similarity between geometric objects is a fundamental problem in many areas of science and engineering. Applications arise e.g., when studying animal behaviour, human movement, traffic management, surveillance and security, military and battlefield, sports scene analysis, and movement in abstract spaces [9, 10, 11]. Due to its practical relevance, the resulting algorithmic problem of curve matching has become one of the well-studied problems in computational geometry. One of the prominent measures of similarities between curves is given by the *Fréchet distance* and its variants.

In the well-known dog-leash metaphor, the (standard) *Fréchet distance* is described as follows: suppose a person walks a dog, while both have to move from the starting point to the ending point on their respective curves T_1 and T_2. Each pair of walks induces a matching between T_1 and T_2. The *Fréchet* distance is the minimum leash length required over all possible pairs of walks, if neither person nor dog is allowed to move backwards.

In this paper, we study the integral and average Fréchet distance originally introduced by Buchin [4]. The *integral Fréchet distance* is defined as the minimal integral of the distances between points that are matched by a pair of walks. The *average Fréchet distance* is defined as the integral Fréchet distance divided by the sum of the lengths of T_1 and T_2.

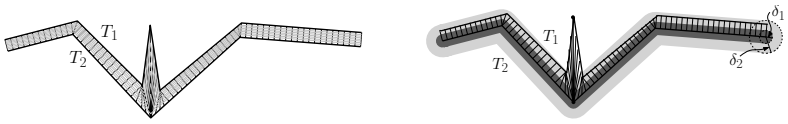

Figure 1 Left: A matching between T_1 and T_2. Right: The partial Fréchet similarity is unstable for distance thresholds between δ_1 and δ_2 where $\delta_1 \approx \delta_2$. In particular, for a leash length of δ_1, the partial Fréchet similarity of T_1 and T_2 is equal to zero, whereas for a leash length of δ_2, it is close to $|T_1| + |T_2|$. Furthermore, the traditional Fréchet distance is significantly enlarged by the peak of T_1.

1.1 Related Work

Alt and Godau [1] showed how to compute the Fréchet distance between two polygonal curves T_1 and T_2 in $\mathcal{O}(n^2 \log(n))$ time, where n is the complexity of T_1 and T_2. In the presence of outliers though, the Fréchet distance may not provide an appropriate result. This is due to the fact that the Fréchet distance measures the maximum of the matched distances. Thus, one large "peak" may substantially increase the Fréchet distance, see Figure 1 left.

To overcome the issue of outliers, Buchin et al. [3] introduced the *partial Fréchet similarity* and showed how to compute it in $\mathcal{O}(n^3 \log(n))$ time, where distances are measured w.r.t. the L_1 or L_∞ metric. The partial Fréchet similarity measures the cost of a matching as the lengths of the parts of T_1 and T_2 which are made up of matched point pairs whose distance to each other is upper-bounded by a given threshold $\delta \geq 0$, see Figure 1 right. De Carufel et al. [5] showed that the partial Fréchet similarity w.r.t. to the L_2 metric cannot be computed exactly over the rational numbers. Motivated by that, they gave a $(1 \pm \varepsilon)$-approximation algorithm guaranteeing a pseudo-polynomial running time. An alternative perspective on the partial Fréchet similarity is the partial Fréchet dissimilarity, i.e., the minimization of the portions on T_1 and T_2 which are involved in distances that are larger than δ.

Unfortunately, both the partial Fréchet similarity and dissimilarity are highly dependent on the choice of δ as provided by the user. As a function of δ, the partial Fréchet distance is unstable, i.e., arbitrarily small changes of δ can result in arbitrarily large changes of the partial Fréchet (dis)similarly, see Figure 1 right.

An approach related to the integral Fréchet distance is dynamic time warping (DTW), which arose in the context of speech recognition [12]. Here, a discrete version of the integral Fréchet distance is computed via dynamic programming. This is not suitable for general curve matching (see [7, p. 204]). Efrat et al. [7] worked out an extension of the idea of DTW to a continuous version. In particular, they compute shortest path distances on a combinatorial piecewise linear 2-manifold that is constructed by taking the Minkowski sum of T_1 and T_2. Furthermore, they gave two approaches dealing with that manifold. The first one does not yield an approximation of the integral Fréchet distance. The second one does not lead to theoretically provable guarantees.

1.2 Contributions

We present the first (pseudo-)polynomial time algorithm that approximates the integral Fréchet Distance, $\mathcal{F}_S(T_1, T_2)$, up to a multiplicative error of $(1 + \varepsilon)$.

As a by-product, we show that a shortest weighted path π_{ab} between two points a and b inside a parameter cell C can be computed in constant time. We also make the observation that π_{ab} provides an optimal matching for the partial Fréchet similarity for all leash length thresholds. This provides a natural extension of locally correct Fréchet matchings that were first introduced by Buchin et al. [2]. They suggest to: “restrict to the locally correct matching

that decreases the matched distance as quickly as possible."[2, p. 237]. The matching induced by π_{ab} fulfils this requirement.

2 Preliminaries

Let $T_1, T_2 : [0, n] \to \mathbb{R}^2$ be two polygonal curves. We denote the first derivative of a function f by f'. By, $||\cdot||_p$, we denote the p-norm and by $d_p(\cdot,\cdot)$ its induced L_p metric. The *lengths* $|T_1|$ *and* $|T_2|$ of T_1 and T_2 are defined as $\int_0^n ||(T_1)'(t)||_2\, dt$ and $\int_0^n ||(T_2)'(t)||_2\, dt$, respectively. To simplify the exposition, we assume that $|T_1| = |T_2| = n$ and that T_1 and T_2 each have n segments. A *reparametrization* is a continuous function $\alpha : [0, n] \to [0, n]$ with $\alpha(0) = 0$ and $\alpha(n) = n$. A reparameterization α is *monotone* if $\alpha(t_1) \leq \alpha(t_2)$ holds for all $0 \leq t_1 \leq t_2 \leq n$. A *(monotone) matching* is a pair of (monotone) reparametrizations (α_1, α_2). The *Fréchet distance* of T_1 and T_2 w.r.t. d_2 is defined as $\mathcal{D}(T_1, T_2) = \inf_{(\alpha_1,\alpha_2)} \max_{t\in[0,n]} d_2(T_1(\alpha_1(t)), T_2(\alpha_2(t)))$.

For a given leash length $\delta \geq 0$, Buchin et al. [3] define the *partial Fréchet similarity* $\mathcal{P}_{(\alpha_1,\alpha_2)}(T_1, T_2)$ *w.r.t. a matching* (α_1, α_2) as

$$\int_{d_2(T_1(\alpha_1(t)),T_2(\alpha_2(t)))\leq\delta} \left(||\left(T_1 \circ \alpha_1\right)'(t)||_2 + ||\left(T_2 \circ \alpha_2\right)'(t)||_2\right) dt$$

and the *partial Fréchet similarity* as $\mathcal{P}_\delta(T_1, T_2) = \sup_{\alpha_1,\alpha_2} \mathcal{P}_{(\alpha_1,\alpha_2)}(T_1, T_2)$.

Given a monotone matching (α_1, α_2), the *integral Fréchet distance* $\mathcal{F}_{\mathcal{S},(\alpha_1,\alpha_2)}(T_1, T_2)$ *of* T_1 *and* T_2 *w.r.t.* (α_1, α_2) is defined as:

$$\int_0^n d_2(T_1(\alpha_1(t)), T_2(\alpha_2(t)))\left(||\left(T_1 \circ \alpha_1\right)'(t)||_2 + ||\left(T_2 \circ \alpha_2\right)'(t)||_2\right) dt$$

and the *integral Fréchet distance* as $\mathcal{F}_\mathcal{S}(T_1, T_2) = \inf_{(\alpha_1,\alpha_2)} \mathcal{F}_{\mathcal{S},(\alpha_1,\alpha_2)}(T_1, T_2)$ [4]. Note that the derivatives of $(T_1 \circ \alpha_1)(\cdot)$ and $(T_2 \circ \alpha_2)(\cdot)$ are measured w.r.t. the L_2-norm because the lengths of T_1 and T_2 are measured in Euclidean space. Furthermore, $(T_1 \circ \alpha_1)'(t)$ and $(T_1 \circ \alpha_1)'(t)$ are well defined for all $t \in [0, n]$ because $(T_1 \circ \alpha_1)'(\cdot)$ and $(T_1 \circ \alpha_1)'(\cdot)$ are piecewise continuously differentiable. The *average Fréchet distance* is defined as $\mathcal{F}_S(T_1, T_2)/(|T_1| + |T_2|)$ [4].

The *parameter space* P of T_1 and T_2 is an axis aligned rectangle. The bottom-left corner $\mathfrak{s}$ and upper-right corner $\mathfrak{t}$ correspond to $(0, 0)$ and (n, n), respectively. We denote the x- and the y-coordinate of a point $a \in P$ by $a.x$ and $a.y$, respectively. A point $b \in P$ *dominates* a point $a \in P$, denoted by $a \leq_{xy} b$, if $a.x \leq b.x$ and $a.y \leq b.y$ hold. A path π is *(xy-) monotone* if $\pi(t_1) \leq \pi(t_2)$ holds for all $0 \leq t_1 \leq t_2 \leq n$. Thus, a monotone matching corresponds to a monotone path π with $\pi(0) = \mathfrak{s}$ and $\pi(n) = \mathfrak{t}$. By inserting $n+1$ vertical and $n+1$ horizontal *parameter lines*, we refine P into n rows and n columns such that the i-th row (column) has a height (resp., width) that corresponds to the length of the i-th segment on T_1 (resp., T_2). This induces a partitioning of P into cells, called *parameter cells*.

For $a, b \in P$ with $a \leq_{xy} b$, we have $||ab||_1 = \int_{a.x}^{b.x} ||(T_1)'(t)||_2\, dt + \int_{a.y}^{b.y} ||(T_2)'(t)||_2\, dt$. This is equal to the sum of the lengths of the subcurves between $T_1(a.x)$ and $T_1(b.x)$ and between $T_2(a.y)$ and $T_2(b.y)$. Thus, we define the *length* $|\pi|$ *of a path* $\pi : [0, n] \to P$ as $\int_0^n ||(\pi)'(t)||_1\, dt$. Note that for the paths inside the parameter space the 1-norm is applied, while the lengths of the curves in the Euclidean space are measured w.r.t. the 2-norm. As $\mathcal{F}_S(T_1, T_2)$ measures the length of T_1 and T_2 at which each $(T_1(\alpha_1(t)), T_2(\alpha_2(t)))$ is weighted by $d_2(T_1(\alpha_1(t)), T_2(\alpha_2(t)))$, we consider the *weighted length* of π defined as follows:

Let $w(\cdot) : P \to \mathbb{R}_{\geq 0}$ be defined as $w((x, y)) := d_2(T_1(x), T_2(y))$ for all $(x, y) \in P$. The weighted length $|\pi|_w$ of a path $\pi : [a, b] \to P$ is defined as $\int_a^b w(\pi(t))\, ||(\pi)'(t)||_1 dt$.

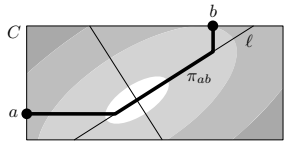

Figure 2 A weighted shortest xy-monotone path π_{ab} between two points $a, b \in C$, where $a \leq_{xy} b$.

▶ **Observation 1** ([4]). *Let π be a shortest weighted monotone path between $\mathfrak{s}$ and $\mathfrak{t}$ inside P. Then, we have $|\pi|_w = \mathcal{F}_{\mathcal{S}}(T_1, T_2)$.*

Motivated by Observation 1, we approximate $\mathcal{F}_S(T_1, T_2)$ by approximating the length of a shortest weighted monotone path $\pi \subset P$ connecting $\mathfrak{s}$ and $\mathfrak{t}$. Let $\delta \geq 0$ be chosen arbitrarily, but fixed. Inside each parameter cell C, the union of all points p with $w(p) \leq \delta$ is equal to the intersection of an ellipse $\mathcal{E}$ with C. Observe that $\mathcal{E}$ can be computed in constant time [1]. $\mathcal{E}$ is characterized by two focal points F_1 and F_2 and a radius r such that $\mathcal{E} = \{p \in \mathbb{R}^2 \mid d_2(p, F_1) + d_2(p, F_2) \leq r\}$. The two axes ℓ (monotone) and $\hbar$ (not monotone) of $\mathcal{E}$, called the *free space axes*, are defined as the line induced by F_1 and F_2 and the bisector between F_1 and F_2. If $\mathcal{E}$ is a disc, ℓ and $\hbar$ are the lines with gradients 1 and -1 and which cross each other in the middle of $\mathcal{E}$. Note that the axes are independent of the value of δ.

To approximate $|\pi|_w$ efficiently we make the following observation that is of independent interest: Let a, b be two parameter points that lie in the same parameter cell C such that $a \leq_{xy} b$. The shortest weighted monotone path π_{ab} between a and b (that induces an optimal solution for the integral Fréchet distance) is the monotone path between a and b that maximizes its subpaths that lie on ℓ (see Figure 2 and Lemma 7). Another interesting aspect of π_{ab} is that it also provides an optimal matching for the partial Fréchet similarity (between the corresponding (sub-)segments) for all leash lengths, as $\pi \cap \mathcal{E}_\delta$ has the maximal length for all $\delta \geq 0$, where $\mathcal{E}_\delta := \mathcal{E}$ for a specific $\delta \geq 0$. Next, we discuss our algorithms.

3 An Algorithm for Approximating Integral Fréchet Distance

We approximate the length of a shortest weighted monotone path between $\mathfrak{s}$ and $\mathfrak{t}$ as follows: We construct two weighted, directed, graphs $G_1 = (V_1, E_1, w_1)$ and $G_2 = (V_2, E_2, w_2)$ that lie embedded in P such that $\mathfrak{s}, \mathfrak{t} \in V_1$ and $\mathfrak{s}, \mathfrak{t} \in V_2$. Then, in parallel, we compute for G_1 and G_2 the lengths of the shortest weighted paths between $\mathfrak{s}$ and $\mathfrak{t}$. Finally, we output the minimum of both values as an approximation for $\mathcal{F}_S(T_1, T_2)$.

We introduce some additional terminology. A *geometric graph* $G = (V, E)$ is a graph where each $v \in V$ is assigned to a point $p_v \in P$, its *embedding*. The *embedding* of an edge $(u, v) \in E$ (into P) is $p_u p_v$. The *embedding of G (into P)* is $\bigcup_{(u,v)\in E} p_u p_v$. For $v \in V$ and $e \in E$, we denote simultaneously the vertex $v \in V$, the edge $e \in E$, and the graph (V, E) and their embeddings by v, e, and G, respectively. G is *monotone (directed)* if $p_u \leq_{xy} p_v$ holds for all $(u, v) \in E$. Let $R \subseteq P$ be an arbitrarily chosen axis aligned rectangle with height h and width b. The *grid (graph) of R with mesh size σ* is the geometric graph that is induced by the segments that are given as the intersections of R with the following lines: Let $h_1, \ldots, h_{k_1}$ be the $\lceil \frac{h}{\sigma} \rceil + 1$ equidistant horizontal lines and let $b_1, \ldots, b_{k_2}$ be the $\lceil \frac{b}{\sigma} \rceil + 1$ equidistant vertical lines such that $\partial R = R \cap (h_1 \cup h_{k_1} \cup b_1 \cup b_{k_2})$, where ∂R denotes the boundary of R.

3.1 Construction of G_1

Let μ be the length of a smallest segment from T_1 and T_2. We construct $G_1 = (V_1, E_1) \subset P$ as the monotone directed grid graph of P with a mesh size of $\frac{\varepsilon\mu^2}{40000(|T_1|+|T_2|)}$. Furthermore, we set $w_1((u,v)) := |uv|_w$ for all $(u,v) \in E_1$.

3.2 Construction of G_2

For $u \in P$ and $r \geq 0$, we consider the ball $B_r(u)$ with its center at u and a radius of r w.r.t. the L_∞ metric. For the construction of G_2 we need the free space axes of the parameter cells and so called grid balls:

▶ **Definition 2.** Let $u \in P$ and $r \geq 0$ be chosen arbitrarily. The *grid ball* $G_r(u)$ is defined as the grid of $B_r(u)$ that has a mesh size of $\frac{\varepsilon}{456}w(u)$. We say $G_r(u)$ *approximates* $B_r(u)$.

We define G_2 as the monotone directed graph that is induced by the arrangement that is made up of the following components restricted to P:

- (1) All monotone free space axes restricted to their corresponding parameter cell.
- (2) All grid balls $G_{62w(u)}(u)$ for $u := \arg\min_{p \in e} w(u)$ and any parameter edge e.
- (3) The segments $\mathfrak{s}c_\mathfrak{s}$ and $\mathfrak{t}c_\mathfrak{t}$ if the parameter cells $C_\mathfrak{s}$ and $C_\mathfrak{t}$ that contain $\mathfrak{s}$ and $\mathfrak{t}$ are intersected by their corresponding monotone free space axes $\ell_\mathfrak{s}$ and $\ell_\mathfrak{t}$, where $c_\mathfrak{s}$ and $c_\mathfrak{t}$ are defined as the bottom-leftmost and top-rightmost point of $\ell_\mathfrak{s} \cap C_\mathfrak{s}$ and $\ell_\mathfrak{t} \cap C_\mathfrak{t}$.

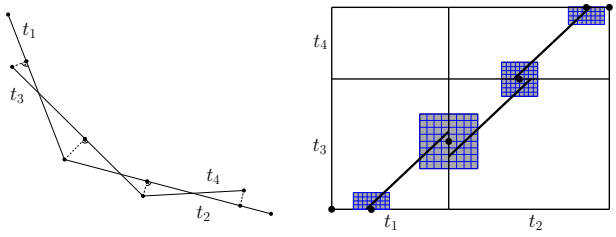

Figure 3 Exemplified construction of G_2 for two given polygonal curves T_1 and T_2. For simplicity, we only illustrate four grid balls (with reduced radii) and the corresponding point pairs from $T_1 \times T_2$.

Finally, we set $w_2((v_1,v_2)) := |v_1v_2|_w$ for all $(v_1,v_2) \in E_2$. For each edge $e \in G_2$, we choose the point $u \in e$ as the center of the corresponding grid ball because the free space axes of the parameters cells adjacent to e lie close to u.

We analyze our approach as follows: Since G_1 is monotone and each edge $(p_1,p_2) \in E_1$ is assigned to $|p_1p_2|_w$, we obtain that for each path it holds that $\widetilde{\pi} \subset G_1$ between $\mathfrak{s}$ and $\mathfrak{t}$ holds $|\pi|_w \leq |\widetilde{\pi}|_w$. The same argument applies to G_2. Hence, we still have to ensure that there is a path $\widetilde{\pi} \subset G_1$ or $\widetilde{\pi} \subset G_2$ such that $|\widetilde{\pi}|_w \leq (1+\varepsilon)|\pi|_w$. We say that a path $\pi \subset P$ is *low* if $w(p) \leq \frac{\mu}{100}$ holds for all $p \in \pi$. For our analysis, we show the following:

- Case A: There is a $\widetilde{\pi} \subset G_1$ with $|\widetilde{\pi}|_w \leq (1+\varepsilon)|\pi|_w$ if there is a shortest path $\pi \subset P$ that is not low (see Section 3.3).
- Case B: Otherwise, there is a $\widetilde{\pi} \subset G_2$ with $|\widetilde{\pi}|_w \leq (1+\varepsilon)|\pi|_w$ (see Section 3.4).

3.3 Analysis of Case A

In this section, we assume that there is a shortest path π between $\mathfrak{s}$ and $\mathfrak{t}$ that is not low. Furthermore, for any $o,p \in \pi$, we denote the subpath of π which is between o and p by π_{op}.

First, we prove a lower bound for $|\pi|_w$ (Lemma 5). This lower bound ensures that the approximation error that we make for a path in G_1 is upper-bounded by $\varepsilon|\pi|_w$ (Lemma 6).

A *cell* C *of* G_1 is the convex hull of four vertices $v_1, v_2, v_3, v_4 \in V_1$ such that $C \cap V_1 = \{v_1, v_2, v_3, v_4\}$. As the mesh size of G_1 is $\frac{\varepsilon\mu^2}{40000(|T_1|+|T_2|)}$, we have $d_1(p_1, p_2) \leq \frac{\varepsilon\mu^2}{20000(|T_1|+|T_2|)}$ for any two points p_1 and p_2 that lie in the same cell of G_1. The following property of $w(\cdot)$ is the key in the analysis of the weighted shortest path length of G_1:

▶ **Definition 3** ([8]). $f : P \to \mathbb{R}_{\geq 0}$ is 1-Lipschitz if $f(x) \leq f(y) + d_1(x, y)$ for all $x, y \in P$.

The requirement $|f(x) - f(y)| \leq d_1(x, y)$ is also occasionally used to define 1-Lipschitz continuity. Note that this alternative definition is equivalent to Definition 3.

▶ **Lemma 4.** *$w(\cdot)$ is 1-Lipschitz.*

Proof. Let $(a_1, a_2), (b_1, b_2) \in P$ be chosen arbitrarily. The subcurves $t_{T_1(a_1)T_1(b_1)} \subset T_1$ between $T_1(a_1)$ and $T_1(b_1)$ and $t_{T_2(a_2)T_2(b_2)} \subset T_2$ between $T_2(a_2)$ and $T_2(b_2)$ have lengths no larger than $|a_1 - b_2|$ and $|a_2 - b_2|$. Thus, $d_2(T_1(a_1), T_1(b_1)) \leq |a_1 - b_1|$ and $d_2(T_2(a_2), T_2(b_2)) \leq |a_2 - b_2|$. Furthermore, $w((a_1, a_2))$ is equal to $d_2(T_1(a_1), T_2(a_2))$. By triangle inequality, it follows that $w((b_1, b_2)) = d_2(T_1(b_1), T_2(b_2)) \leq d_2(T_2(b_2), T_2(a_2)) + d_2(T_2(a_2), T_1(a_1)) + d_2(T_1(a_1), T_1(b_1)) \leq d_1((a_1, a_2), (b_1, b_2)) + w((a_1, a_2))$, because $d_2(T_2(b_2), T_2(a_2)) = |b_2 - a_2|$, $d_2(T_2(a_2), T_1(a_1)) = w((a_1, a_2))$, $d_2(T_1(a_1), T_1(b_1)) = |b_1 - a_1|$, and $d_1((a_1, a_2), (b_1, b_2)) = |b_1 - a_1| + |b_2 - a_2|$. ◀

Lemma 4 allows us to prove the following lower bound for the weighted length of π.

▶ **Lemma 5.** $|\pi|_w \geq \frac{\mu^2}{20000}$.

Proof. Let $p \in \pi$ such that $w(p) \geq \frac{\mu}{100}$. Let $\psi := \pi \cap B_{\frac{\mu}{100}}(p)$. We have $|\psi|_w \geq \frac{\mu^2}{20000}$ because $w(\cdot)$ is 1-Lipschitz. Furthermore, $\psi \subset \pi$ implies $|\psi|_w \leq |\pi|_w$ which yields $\frac{\mu^2}{20000} \leq |\pi|_w$. ◀

▶ **Lemma 6.** *There is a path $\widetilde{\pi} \subset G_1$ that connects $\mathfrak{s}$ and $\mathfrak{t}$ such that $|\widetilde{\pi}|_w \leq (1 + \varepsilon)|\pi|_w$.*

Proof. Starting from $\mathfrak{s}$, we construct $\widetilde{\pi}$ inductively as follows: If π crosses a vertical (horizontal) parameter line next, $\widetilde{\pi}$ goes one step to the right (top). For $p \in \pi$ let h_p be the line with gradient -1 such that $p \in h_p$ (see the figure on the right). As π and $\widetilde{\pi}$ are monotone, the point $\widetilde{p} := h_p \cap \widetilde{p}$ is unique and well defined. For all p, p and $\widetilde{p}$ lie in the same cell of G_1 and thus, $w(\widetilde{p}) \leq w(p) + \frac{\varepsilon\mu^2}{20000(|T_1|+|T_2|)}$. This implies $|\widetilde{\pi}|_w \leq (1 + \varepsilon)|\pi|_w$ because $|\widetilde{\pi}| = |\pi|$. To be more precise, we consider $\widetilde{\pi}, \pi : [0, 1] \to P$ to be parametrized such that $d_1(\mathfrak{s}, \pi(t)) = d_1(\mathfrak{s}, \widetilde{\pi}(t)) = t d_1(\mathfrak{s}, \mathfrak{t})$. We obtain, $||(\widetilde{\pi})'(t)||_1 = d_1(\mathfrak{s}, \mathfrak{t}) = ||(\pi)'(t)||_1$ for all $t \in [0, 1]$.

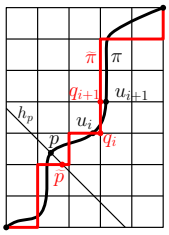

Furthermore, the above implies $w(\widetilde{\pi}(t)) \leq w(\pi(t)) + \frac{\varepsilon\mu^2}{20000(|T_1|+|T_2|)}$ $(\star)$. Thus:

$$\begin{aligned}|\widetilde{\pi}|_w &= \int_0^1 w(\widetilde{\pi}(t))||(\widetilde{\pi})'(t)||_1 \, dt \overset{(\star)}{\leq} \int_0^1 \left(w(\pi(t)) + \frac{\varepsilon\mu^2}{20000(|T_1|+|T_2|)}\right) ||(\pi)'(t)||_1 \, dt \\ &= \int_0^1 w(\pi(t))||(\pi)'(t)||_1 \, dt + \frac{\varepsilon\mu^2 \int_0^1 1 \; ||(\pi)'(t)||_1 \, dt}{20000(|T_1|+|T_2|)} \\ &= |\pi|_w + \frac{\varepsilon\mu^2}{20000} \overset{\text{Lemma 5}}{\leq} |\pi|_w + \varepsilon|\pi|_w = (1+\varepsilon)|\pi|_w.\end{aligned}$$

◀

The proof of Lemma 6 is omitted due to space constraints. All proofs that are omitted or just sketched can be found in the Appendix.

3.4 Analysis of Case B

In this section, we assume that there is a shortest monotone low path π between $\mathfrak{s}$ and $\mathfrak{t}$. First, we make a key observation that is also of independent interest.

▶ **Lemma 7.** *Let C be an arbitrarily chosen parameter cell and $a, b \in C$ such that $a \leq_{xy} b$. Furthermore, let ℓ be the monotone free space axis of C and R the rectangle that is induced by a and b. The shortest path $\pi_{ab} \subset C$ between a and b is given as:*

- *$ac_1 \cup c_1c_2 \cup c_2b$, if ℓ intersects R in c_1 and c_2 such that $c_1 <_{xy} c_2$ and as*
- *$ac \cup cb$, otherwise, where c is defined as the closest point from R to ℓ.*

Proof. Let $\psi_{ab} \subset C$ by an arbitrary monotone path that connects a and b. In the following, we show that $|\pi_{ab}|_w \leq |\psi_{ab}|_w$. For this, we prove the following: Let $p \in C$ be chosen arbitrarily and q be its orthogonal projection onto ℓ (see the figures right). We show $w(r) \leq w(p)$ for $r \in pq$. This implies that there is an injective, continuous function $\perp : \psi_{ab} \to \pi_{ab}$ with $w(\perp(p)) \leq w(p)$ for all $p \in \psi$. In particular, $\perp(p)$ is defined as the intersection point of π_{ab} and the line d that lies perpendicular to ℓ such that $p \in d$. The function $\perp(\cdot)$ is well defined and injective as both ψ_{ab} and π_{ab} are monotone paths that connect a and b. Similarly, as in the proof of Lemma 6, this implies $|\pi_{ab}|_w \leq |\psi_{ab}|_w$ because $|\pi_{ab}| = |\psi_{ab}|$.

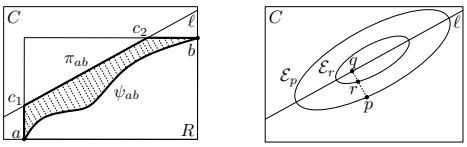

To be more precise, consider $\psi, \pi : [0,1] \to C$ to be parametrized such that $d_1(a, \psi(t)) = d_1(a, \pi(t)) = td_1(a, b)$. This implies $||(\psi)'(t)||_1 = d_1(a, b) = ||(\pi)'(t)||_1$ for all $t \in [0, 1]$. Thus:

$$|\psi_{ab}|_w \quad = \quad \int_0^1 w(\psi_{ab}(t))||(\psi_{ab})'(t)||_1 \, dt \geq \int_0^1 w(\pi_{ab}(t))||(\pi_{ab})'(t)||_1 \, dt = |\pi_{ab}|_w.$$

Finally, we show: $w(r) \leq w(p)$, for $r \in pq$. Note that $w(r)$ and $w(p)$ are the leash lengths for r and p that lie on the boundary of the white space inside C, i.e., on the boundary of the ellipses $\mathcal{E}_r$ and $\mathcal{E}_p$, respectively. Since $r \in pq$ we get $\mathcal{E}_r \subseteq \mathcal{E}_p$, which implies $w(r) \leq w(p)$. ◀

We call a point $p \in C$ *canonical* if $p \in \ell$. Let C_o and C_p be two parameter cells that share a parameter edge e. Furthermore, let $o \in \ell_o \subset C_o$ and $p \in \ell_p \subset C_p$ be two canonical parameter points such that $o \leq_{xy} p$ where ℓ_o and ℓ_p are the monotone free space axis of C_o and C_p, respectively. Let c_o be the top-right end point of ℓ_o and c_p the bottom-left end point of ℓ_p. The following corollary to Lemma 7 characterizes how a shortest path passes through the parameter edges.

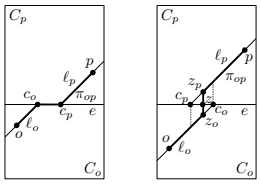

(a) $o \leq_{xy} p$ (b) $o \not\leq_{xy} p$

Figure 4 Configurations of Corollary 8.

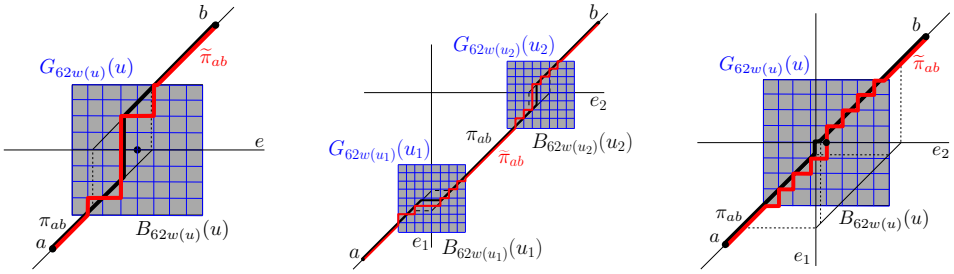

(a) Case (1.) (b) Case (2.1.) (c) Case (2.2.)

Figure 5 Different subcases how π_{ab} is approximated by free space axes and grid balls.

▶ **Corollary 8.** *If $c_o, c_p \in e$ and $c_o \leq_{xy} c_p$, π_{op} is equal to the concatenation of the segments oc_o, c_oc_p, and c_pp (see Figure 4(a) on right). Otherwise, there is a $z \in e$ such that π_{op} is equal to the concatenation of the segments oz_o, z_oz_p, and z_pp, where $z_o \in \ell_{C_o}$ and $z_p \in C_p$ such that z is the orthogonal projection of z_o and z_p onto e (see Figure 4(b)).*

3.4.1 Outline of the analysis of Case B

In the following, we apply Lemma 7 and Corollary 8 to subpaths π_{ab} of π in order to ensure that π_{ab} is a subset of the union of a constant number of balls (that are approximated by grid balls in our approach) and monotone free space axes. In particular, we construct a discrete sequence of points from π which lie on the free space axes, see Section 3.4.2. For each induced subpath π_{ab}, we ensure that π_{ab} crosses one or two perpendicular parameter edges. For the analysis we distinguish between the two cases which we consider separately:

- Case 1: π_{ab} crosses one parameter edge and
- Case 2: π_{ab} crosses two parameter edges.

For Case 1, we show that, if π_{ab} crosses one edge (e) then π_{ab} is a subset of the union of the two monotone free space axes of the parameter cells that share e and the ball $B_{62w(u)}(u)$ for $u := \arg\min_{p \in e} w(u)$ (see Figure 5(a) and Section 3.4.3).

For Case 2, (see Section 3.4.4), we consider the case that π_{ab} crosses two parameter edges e_1 and e_2. In particular, π_{ab} runs through three parameter cells C_q, C_r, and C_s, where C_q and C_r share e_1 and C_r and C_s share e_2.

We further distinguish further between two subcases. For this, let $u_1 := \arg\min_{p \in e_1} w(p)$ and $u_2 := \arg\min_{p \in e_2} w(p)$.

- Case 2.1: We show that, if $d_1(u_1, u_2) \geq 6 \max\{w(u_1), w(u_2)\}$, then π_{ab} is a subset of the union of the balls $B_{62w(u_1)}(u_1)$ and $B_{62w(u_2)}(u_2)$ and the monotone free space axes of C_q, C_r, and C_s (see Figure 5(b) and Lemma 13).
- Case 2.2: We show that, if $d_1(u_1, u_2) \leq 6 \max\{w(u_1), w(u_2)\}$, then π_{ab} is a subset of the union of the ball $B_{62w(u)}(u)$ and the monotone free space axes of C_q and C_s for $u \in \{u_1, u_2\}$ (see Figure 5(c) and Lemma 17).

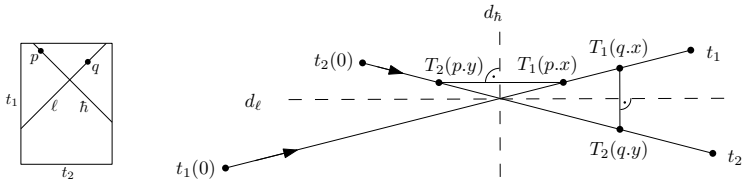

Figure 6 Duality of parameter points from ℓ ($\hbar$) and leashes that lie perpendicular to d_ℓ ($d_\hbar$).

For the analysis of the length of a shortest path $\widetilde{\pi} \subset G_2$ that lies between $\mathfrak{s}$ and $\mathfrak{t}$, we construct for $\pi_{ab} \subset \pi$ a path $\widetilde{\pi}_{ab} \subset G_2$ between a and b such that $|\widetilde{\pi}_{ab}|_w \leq (1+\varepsilon)|\pi_{ab}|_w$. In particular, $\widetilde{\pi}_{ab}$ is a subset of the grid balls that approximate the above considered balls and the free space axes that are involved in the individual (sub-)case for π_{ab} (see, Figure 5). Finally, we define $\widetilde{\pi} \subset G_2$ as the concatenation of the approximations $\widetilde{\pi}_{ab}$ for all π_{ab}.

3.4.2 Separation of a shortest path

In the following, we determine a discrete sequence of canonical points $\mathfrak{s} = p_1, ..., p_k = \mathfrak{t} \in \pi$ such that $\pi_{p_i p_{i+1}}$ crosses at most two parameter lines for each $i \in \{1, ..., k-1\}$. First, we need the following supporting lemma:

▶ **Lemma 9.** *For all $q_1, q_2 \in \pi$ that lie in the same parameter cell with $q_1 \leq_{xy} q_2$ we have $q_2.y - q_1.y - \frac{\mu}{50} \leq q_2.x - q_1.x \leq q_2.y - q_1.y + \frac{\mu}{50}$.*

Proof. By triangle inequality we obtain:
$d_2(T_2(q_2.y), T_2(q_1.y)) \leq d_2(T_2(q_2.y), T_1(q_2.x)) + d_2(T_1(q_2.x), T_1(q_1.x)) + d_2(T_1(q_1.x), T_2(q_1.y))$.
This implies $d_2(T_2(q_2.y), T_2(q_1.y)) - \frac{\mu}{50} \leq d_2(T_1(q_2.x), T_1(q_1.x))$, because $d_2(T_2(q_2.y), T_1(q_2.x)), d_2(T_1(q_1.x), T_2(q_1.x)) \leq \frac{\mu}{100}$. Furthermore, $d_2(T_2(q_2.y), T_2(q_1.y)) = q_2.y - q_1.y$ and $d_2(T_1(q_2.x), T_1(q_1.x)) = q_2.x - q_1.x$ because q_1 and q_2 lie in the same cell. This implies $q_2.y - q_1.y - \frac{\mu}{50} \leq q_2.x - q_1.x$. A corresponding argument yields that $q_2.x - q_1.x \leq q_2.y - q_1.y + \frac{\mu}{50}$. ◀

▶ **Lemma 10.** *There are canonical points $\mathfrak{s} = p_1, \ldots p_k = \mathfrak{t} \in \pi$ such that for all $i \in \{1, \ldots, k-1\}$ the following holds: (P1) $\pi_{p_i p_{i+1}}$ crosses at most one vertical and at most one horizontal parameter line which are both not part of ∂P and (P2) the distance of p_i to a parameter line is lower-bounded by $\frac{\mu}{6}$ for all $i \in \{2, \ldots, k-1\}$.*

3.4.3 Analysis of subpaths that cross one parameter edge

We need to show that those parts of π that do not lie on the free space axes are covered by the balls $B_{62w(u)}$. For this, we use the following geometrical interpretation of the free space axes ℓ and $\hbar$ of a parameter cell C. Let $t_1 \in T_1$ and $t_2 \in T_2$ be the segments that correspond to C. We denote the angular bisectors of t_1 and t_2 by d_ℓ and $d_\hbar$ such that the start points $t_1(0)$ and $t_2(0)$ of t_1 and t_2 lie on different sides w.r.t. $d\ell$, see Figure 6 right. If t_1 and t_2 are parallel, then d_ℓ denotes the line between t_1 and t_2 and we declare $d_\hbar$ as undefined. We observe:

▶ **Observation 11.** *$q \in \ell \Leftrightarrow T_1(q.x)T_2(q.y) \perp d_\ell$ and $p \in \hbar \Leftrightarrow T_1(p.x)T_2(p.y) \perp d_\hbar$.*

From now on, let $o, p \in \pi$ be two consecutive, canonical points that are given via Lemma 10 such that $o \leq_{xy} p$. Furthermore, let ℓ_o and ℓ_p be the free space axes of the parameter cells C_o and C_p such that $o \in \ell_o \subset C_o$ and $p \in \ell_p \subset C_p$.

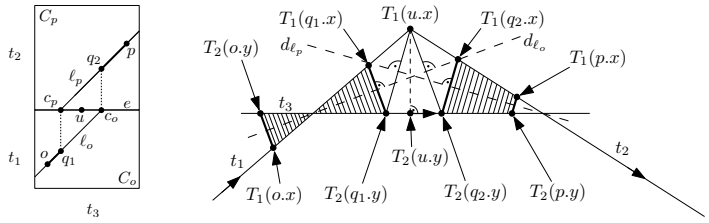

Figure 7 Configuration of the Lemmas 12 and 13: The length of the subpath of π_{op} that does not necessarily lie on $\ell \cup \hbar$ is related to $w(u)$.

▶ **Lemma 12.** *If π_{op} crosses one parameter edge e, points $c_o, c_p \in e$ exist and we have $d_\infty(c_o, c_p) \leq \frac{w(u)}{2}$ where $u = \arg\min_{p \in e} w(p)$.*

Proof. W.l.o.g., we assume that e is horizontal. Let $t_1, t_2 \in T_1$ and $t_3 \in T_2$ be the segments that induce parameter cells C_o and C_p. Below, we show $\angle(t_1, t_3), \angle(t_2, t_3) \leq 7°$ and, then, that $d_1(c_0, c_p) \leq w(u)$. Let $q_1 \in \ell_o$ and $q_2 \in \ell_p$ such that $q_1.x = c_p$ and $q_2.x = c_o$, see Figure 7 left. $\angle(t_1, t_3) \leq 7°$ implies $\angle(T_1(u.x)T_2(u.y), T_1(u.x)T_2(q_2.y)) \leq 3.5°$. Furthermore, $c_p = e \cap \ell_p$ implies: c_p corresponds to a leash $l_p = (T_1(c_p.x), T_2(c_p.y))$ such that $T_1(c_p.x) = T_1(u.x)$ and $T_1(c_p.x), T_2(c_p.y) \perp d_{\ell_o}$, see Figure 7 right. Thus, $d_2(T_2(q_2.y), T_2(u.y))$ is upper-bounded by $d_2(T_2(u.y), T_2(q_2.y)) \leq d_2(T_1(u.x), T_2(u.y)) \tan(3.5°) \leq 0.065 w(u) < \frac{w(u)}{2}$.

Finally, we show that $\angle(t_1, t_3), \angle(t_2, t_3) \leq 7°$. We know that $d_2(T_1(o.x), T_2(o.y))$ and $d_2(T_1(u.x), T_2(u.x))$ are upper-bounded by $\frac{\mu}{100}$ because π is low. Lemma 10 implies $d_2(T_1(o.x), T_1(u.x)), d_2(T_2(o.y), T_2(u.y)) \geq \frac{\mu}{6}$. Thus, $\angle(t_1, t_3) \leq \arcsin \frac{6}{50} \leq 7°$. A similar argument implies that $\angle(t_2, t_3) \leq \arcsin \frac{6}{50} \leq 7°$ ◀

▶ **Lemma 13.** *$\pi_{op} \subset \ell_o \cup B_{w(u)}(u) \cup \ell_p$ (see Figure 5(a)).*

Proof. We combine Corollary 8 and Lemma 12. Corollary 8 implies that π_{op} orthogonally crosses e at a point z that lies between c_o and c_p such that $z \in z_o z_p \subset \pi_{op}$. Lemma 12 implies $d_1(c_o, c_p) \leq \frac{w(u)}{2}$. Thus, $z_o z_p \subset B_{w(u)}(u)$. Furthermore, $o z_o \subset \ell_o$ and $z_p p \subset \ell_p$. This implies $\pi_{op} \subset \ell_o \cup B_{w(u)}(u) \cup \ell_p$ because $\pi_{op} = o z_o \cup z_o z_p \cup z_p p$. ◀

▶ **Lemma 14.** *There is a path $\widetilde{\pi}_{op} \subset G_2$ between o and p such that $|\widetilde{\pi}_{op}|_w \leq (1+\varepsilon)|\pi_{op}|_w$.*

Proof (Sketch). By Lemma 13, the following two intersection points are well defined: Let z_o be the intersection point of ℓ_o and $\partial B_{62w(u)}(u)$ that lies on the left or bottom edge of $\partial B_{62w(u)}(u)$. Analogously, let z_p be the intersection point of ℓ_p and $\partial B_{62w(u)}(u)$ that lies on the right or top edge of $\partial B_{62w(u)}(u)$. By Lemma 13, we can subdivide π_{op} into the three pieces $o z_o \subset \ell_o$, $\pi_{z_o z_p}$, and $z_p p \subset \ell$. As $o z_o, z_p p \subset G_2$, we just have to construct a path $\widetilde{\pi}_{z_o z_p} \subset G_2$ between z_o and z_p such that $|\pi_{z_o z_p}|_w \leq (1+\varepsilon)|\widetilde{\pi}_{z_o z_p}|_w$.

We construct $\widetilde{\pi}_{z_o z_p}$ by applying the same approach as used in the proof of Lemma 6 (see Figure 5(a)). To upper-bound $|\widetilde{\pi}_{z_o z_p}|_w$ by $(1+\varepsilon)|\pi_{z_o z_p}|_w$, we first lower-bound $|\pi_{z_o z_p}|_w$ by $\frac{1}{2}w^2(u)$. By using a similar approach as in the proof of Lemma 6, we can conclude the proof. Further details are provided in the Appendix. Let $\psi := \pi_{z_o z_p} \cap B_{w(u)}(u)$. As $|\psi| \geq w(u)$ and $w(\cdot)$ is 1-Lipschitz, we obtain $|\psi|_w \geq \frac{1}{2}w^2(u)$. Thus, $|\pi_{z_o z_p}|_w \geq \frac{1}{2}w^2(u)$ as $\psi \subset \pi_{z_o z_p}$. ◀

3.4.4 Analysis of subpaths that cross two parameter edges

Let q and s be two consecutive parameter points from $\{p_2, \ldots, p_{k-1}\}$ such that π_{qs} crosses two parameter edges e_1 and e_2. By Lemma 10, e_1 and e_2 are perpendicular to each other and are adjacent at a point c. Let C_r be the parameter cell such that e_1 and e_2 are part of

the boundary of C_r. Furthermore, let C_q and C_s be the parameter cells such that $q \in C_q$ and $s \in C_s$. We denote the monotone free space axis of C_q, C_r, and C_s by ℓ_q, ℓ_r, and ℓ_s, respectively. Let $u_1 := \arg\min_{a \in e_1} w(a)$ and $u_2 := \arg\min_{a \in e_2} w(a)$.

▶ **Lemma 15.** *If $d_1(u_1, u_2) \geq 6\max\{w(u_1), w(u_2)\}$, there is another canonical parameter point $r \in \ell_r$ such that $\pi_{qs} \subset \ell_q \cup B_{w(u_1)}(u_1) \cup \ell_r \cup B_{w(u_2)}(u_2) \cup \ell_s$.*

The proof of Lemma 15 is similar to the proof of Lemma 12.

▶ **Lemma 16.** *If $d_1(u_1, u_2) \geq 6\max\{w(u_1), w(u_2)\}$, then there is a path $\widetilde{\pi}_{qs} \subset G_2$ between q and s such that $|\widetilde{\pi}_{qs}|_w \leq (1+\varepsilon)|\pi_{qs}|_w$.*

Proof. Lemma 15 implies that the following constructions are unique and well defined: Let z_1 (z_2) be the intersection point of $\partial B_{w(u_1)}(u_1)$ and ℓ_q (ℓ_r) that lies on the left or bottom (respectively, right or top) edge of $\partial B_{w(u_1)}(u_1)$. Analogously, let z_3 (z_4) be the intersection point of $\partial B_{w(u_2)}(u_2)$ and ℓ_r (ℓ_s) that lies on the left or bottom (respectively, right or top) edge of $\partial B_{w(u_2)}(u_2)$. By applying the approach of Lemma 14, for $\pi_{z_1 z_2}$ and $\pi_{z_3 z_4}$, we obtain a path $\widetilde{\pi}_{z_1 z_2} \subset G_2$ between z_1 and z_2 and a path $\widetilde{\pi}_{z_3 z_4} \subset G_2$ between z_3 and z_4 such that $|\widetilde{\pi}_{z_1 z_2}|_w \leq (1+\varepsilon)|\pi_{z_1 z_2}|_w$ and $|\widetilde{\pi}_{z_3 z_4}|_w \leq (1+\varepsilon)|\pi_{z_3 z_4}|_w$. This concludes the proof because $qz_1, z_2 z_3, z_4 s \subset G_2$. ◀

▶ **Lemma 17.** *If $d_1(u_1, u_2) \leq 6\max\{w(u_1), w(u_2)\}$, then $\pi_{qs} \subset \ell_q \cup B_{62w(u)\}}(u) \cup \ell_s$ where $u := \arg\max_{u \in \{u_1, u_2\}}\{w(u_1), w(u_2)\}$.*

Lemma 17 implies that the approach taken in the proof of Lemma 14 yields that there is a path $\widetilde{\pi}_{qs} \subset G_2$ between q and s such that $|\widetilde{\pi}_{qs}|_w \leq (1+\varepsilon)|\pi_{qs}|_w$ If $d_1(u_1, u_2) < 6\max\{w(u_1), w(u_2)\}$. Combining this with Lemmas 14 and 16 yields the following corollary:

▶ **Corollary 18.** *Let $\widetilde{\pi} \subset G_2$ be a shortest path. We have $|\pi|_w \leq |\widetilde{\pi}|_w \leq (1+\varepsilon)|\pi|_w$.*

3.5 "Bringing it all together"

In Sections 3.3 and 3.4, we proved that in Cases A and B, the minimum of the shortest path lengths in G_1 and G_2 is no larger than $(1+\varepsilon)|\pi|_w$, where π_w is a shortest path in P.

Next, we discuss that our algorithm has a running time of $\mathcal{O}(\frac{\zeta^4 n^4}{\varepsilon})$. Graph G_1 is given by the arrangement that is induced by $\Theta(\frac{\zeta^2 n^2}{\varepsilon})$ horizontal and $\Theta(\frac{\zeta^2 n^2}{\varepsilon})$ vertical lines because the corresponding grid has a mesh of size $\frac{\varepsilon \mu^2}{40000(|T_1|+|T_2|)}$. Thus, $|E_1| \in \Theta(\frac{\zeta^4 n^4}{\varepsilon^2})$. Graph G_2 is given by the arrangement that is induced by $\mathcal{O}(n^2)$ free space axis and $\Theta(n^2)$ grid balls. Each grid ball has a complexity of $\Theta(\frac{1}{\varepsilon})$. Thus, $|E_2| \in \mathcal{O}(\frac{n^4}{\varepsilon^2})$. Applying Dijkstra's shortest path algorithm on G_1 and G_2 takes time proportional to $\mathcal{O}(|E_1|)$ and $\mathcal{O}(|E_2|)$. As $|E_1| \in \Theta(\frac{\zeta^4 n^4}{\varepsilon^2})$ and $|E_2| \in \mathcal{O}(\frac{n^4}{\varepsilon^2})$ we have to ensure that each edge of $E_1 \cup E_2$ can be computed in constant time to guarantee an overall running time of $\mathcal{O}(\frac{\zeta^4 n^4}{\varepsilon^2})$.

▶ **Lemma 19.** *All edges of G_1 and G_2 can be computed in $\mathcal{O}(1)$ time.*

This leads to our main result.

▶ **Theorem 20.** *We can compute an $(1+\varepsilon)$-approximation of $\mathcal{F}_{\mathcal{S}}(T_1, T_2)$ in $\mathcal{O}(\frac{\zeta^4 n^4}{\varepsilon^2})$ time.*

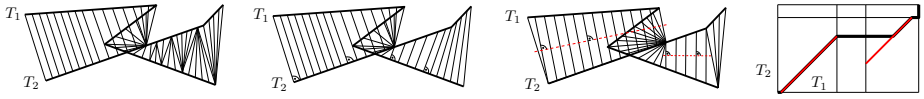

Figure 8 First: The definition of local correctness still allowes "unnatural" matchings. Second: A lexicographic matching. Third: A locally optimal matching that is also optimal w.r.t. integral Fréchet distance. Fourth: The shortest path $\pi \subset P$ (black) that corresponds to the third matching.

4 Locally optimal Fréchet matchings

In this section, we discuss an application of our observations regarding free space axes to so-called *locally correct (Fréchet) matchings* (α_1, α_2) as introduced by Buchin et al. [2]. For $i \in \{1, 2\}$ and $0 \leq a \leq b \leq n$, we denote the subcurve between $T_i(a)$ and $T_i(b)$ by $T_i[a, b]$.

▶ **Definition 21** ([2]). (α_1, α_2) is *locally correct* if $\mathcal{D}\left(T_1[\alpha_1(a), \alpha_2(b)], T_2[\alpha_1(a), \alpha_2(b)]\right) = \max_{t \in [\alpha_1(a), \alpha_2(b)]} d_2(T_1(t), T_2(t))$, for all $0 \leq a \leq b \leq n$.

Buchin et al. [2] suggested to extend the definition of locally correct matchings to "locally optimal" matchings as a future work. "The idea is to restrict to the locally correct matching that decreases the matched distance as quickly as possible."[2, p. 237].

Rote [13] proposed such an extension in terms of the *profile* of a matching. Roughly speaking, the profile of a matching measures, for each threshold $\delta \geq 0$, the amount of time that $d_2(T_1(\alpha_1), T_2(\alpha_2))$ is at least δ. Based on matchings' profiles, Rote defined an order of matchings by applying the *lexicographic order* of their profiles. Without any further restrictions, the lexicographic order of matchings does not make sense because "otherwise we could simply traverse the two curves at a larger speed and accordingly scale down the profile of the considered matching."[13]. Thus, Rote assumes additionally that the "speed at which the curves are traversed by parametrizations is bounded by 1"[13].

Rote [13] gives an algorithm to compute a lexicographic matching in $\mathcal{O}\left(n^3 \log n\right)$ time.

In contrast to [13], we do not measure time w.r.t. the integral of parameter values but w.r.t. the length of traversed subcurves. This has the advantage that we do not need an additional restriction to the considered matchings because the lengths of traversed subcurves is invariant w.r.t. the speed in that they are traversed. In the following, we give a corresponding definition of simply computable locally optimal matchings.

Let (α_1, α_2) be a locally correct matching. As the function $f : t \mapsto d_2(T_1(\alpha_1(t)), T_2(\alpha_2(t)))$ is in general not monotone, we ask for a matching that locally increases and decreases the leash length between two maxima "as fast as possible". In particular, we measure speed in terms of the lengths of subcurves being traversed to achieve a required leash length.

More formally, $t \in [0, n]$ is the *parameter of a local maxima* of f if there is a $\delta_t > 0$ such that for all $0 \leq \delta \leq \delta_t : f(t \pm \delta) \leq f(t)$ and $f(t + \delta) < f(t)$ or $f(t - \delta) < f(t)$. For any $t_1, t_2 \in [0, n]$ and $i \in \{1, 2\}$, we denote the restriction of α_i to $[t_1, t_2]$ as $\alpha_i[t_1, t_2]$.

▶ **Definition 22.** (α_1, α_2) is locally optimal if $\mathcal{P}_\delta(T_1[\alpha_1(t_1), \alpha_1(t_2)], T_2[\alpha_2(t_1), \alpha_2(t_2)]) = \mathcal{P}_{(\alpha_1[t_1,t_2], \alpha_2[t_1,t_2])}(T_1, T_2)$ for all $\delta \geq 0$ and for all parameters of local maxima $t_1, t_2 \in [0, n]$ such that $[t_1, t_2]$ does not contain any further parameter of a local maximum.

By applying a similar approach as in the proof of Lemma 7 we obtain the following:

▶ **Lemma 23.** *Let C be an arbitrarily chosen parameter cell and $a, b \in C$ such that $a \leq_{xy} b$ and π_{ab} the path induced by Lemma 7. Then, $\mathcal{P}_\delta(T_1[a.x, b.x], T_2[a.y, b.y]) = |\mathcal{E}_\delta \cap \pi_{ab}|$ for all $\delta \geq 0$, where $\mathcal{E}_\delta$ is the free space ellipse of C for the distance threshold δ.*

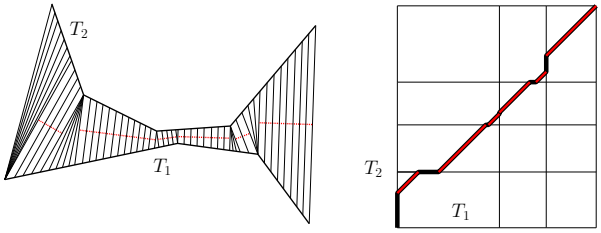

Figure 9 Left: A locally optimal matching that is also global optimal w.r.t. integral Fréchet distance and partial Fréchet similarity for any $\delta \geq 0$. Right: The shortest path that corresponds to the matching to the left. Following completely the free space axes is allowed because the end points of the free space axes can be ordered w.r.t. xy-monotonicity.

Lemma 23 implies the following:

▶ **Corollary 24.** *A locally correct matching can be transformed into a locally optimal Fréchet matching in $\mathcal{O}(n)$. Generally, a locally optimal matching can be computed in $\mathcal{O}(n^3 \log n)$.*

Proof. Let $\pi \subset P$ be the path that corresponds to the locally correct matching. Furthermore, let $p_1, \ldots, p_{2n} \in \pi$ be the intersection points of π with the parameter grid. For each $i \in \{1, ..., 2n-1\}$ we substitute the subpath $\pi_{p_i p_{i+1}}$ by the path between p_i and p_{i+1} which is induced by Lemma 7. The algorithm from [2] computes a locally correct matching in $\mathcal{O}(n^3 \log n)$ time. Thus, a locally optimal matching can be computed in $\mathcal{O}(n^3 \log n)$ time. ◀

5 Conclusion

We presented a pseudo-polynomial $(1+\varepsilon)$-approximation algorithm for the integral and average Fréchet distance which has a running time of $\mathcal{O}(\frac{\zeta^4 n^4}{\varepsilon^2})$. In particular, in our approach we compute two geometric graphs and their weighted shortest path lengths in parallel. It remains open if one can reduce the complexity of G_1 to polynomial with respect to the input parameters such that using $G_1 \cup G_2$ still ensures an $(1+\varepsilon)$-approximation.

As a byproduct we developed techniques to determine the local nature of an optimal matching (α_1, α_2) (without any further restrictions to (α_1, α_2)) w.r.t. different Fréchet measures. It remains open how these techniques can be extended such that not only local, but global optimal matchings can be computed. See Figure 9 for an example. We are currently investigating this extension.

References

1 Helmut Alt and Michael Godau. Computing the Fréchet distance between two polygonal curves. *Int. J. Comput. Geometry Appl.*, 5:75–91, 1995. doi:10.1142/S0218195995000064.

2 Kevin Buchin, Maike Buchin, Wouter Meulemans, and Bettina Speckmann. Locally correct Fréchet matchings. In Leah Epstein and Paolo Ferragina, editors, *ESA*, volume 7501 of *Lecture Notes in Computer Science*, pages 229–240. Springer, 2012. doi:10.1007/978-3-642-33090-2_21.

3 Kevin Buchin, Maike Buchin, and Yusu Wang. Exact algorithms for partial curve matching via the Fréchet distance. In Claire Mathieu, editor, *SODA*, pages 645–654. SIAM, 2009. doi:10.1137/1.9781611973068.

4 Maike Buchin. On the computability of the Fréchet distance between triangulated surfaces. Ph.D. thesis, Dept. of Comput. Sci., Freie Universität, Berlin, 2007.

5 Jean-Lou De Carufel, Amin Gheibi, Anil Maheshwari, Jörg-Rüdiger Sack, and Christian Scheffer. Similarity of polygonal curves in the presence of outliers. *Comput. Geom.*, 47(5):625–641, 2014.

6 Isabel F. Cruz, Craig A. Knoblock, Peer Kröger, Egemen Tanin, and Peter Widmayer, editors. *SIGSPATIAL 2012 International Conference on Advances in Geographic Information Systems (formerly known as GIS), SIGSPATIAL'12, Redondo Beach, CA, USA, November 7-9, 2012*. ACM, 2012.

7 Alon Efrat, Quanfu Fan, and Suresh Venkatasubramanian. Curve matching, time warping, and light fields: New algorithms for computing similarity between curves. *Journal of Mathematical Imaging and Vision*, 27(3):203–216, 2007. doi:10.1007/s10851-006-0647-0.

8 Stefan Funke and Edgar A. Ramos. Smooth-surface reconstruction in near-linear time. In *Proceedings of the Thirteenth Annual ACM-SIAM Symposium on Discrete Algorithms, January 6-8, 2002, San Francisco, CA, USA.*, pages 781–790, 2002.

9 Joachim Gudmundsson, Patrick Laube, and Thomas Wolle. Movement patterns in spatio-temporal data. In Shashi Shekhar and Hui Xiong, editors, *Encyclopedia of GIS*, pages 726–732. Springer, 2008. doi:10.1007/978-0-387-35973-1_823.

10 Joachim Gudmundsson and Nacho Valladares. A GPU approach to subtrajectory clustering using the Fréchet distance. In Cruz et al. [6], pages 259–268. doi:10.1145/2424321.2424355.

11 Joachim Gudmundsson and Thomas Wolle. Football analysis using spatio-temporal tools. In Cruz et al. [6], pages 566–569. doi:10.1145/2424321.2424417.

12 Lawrence R. Rabiner and Biing-Hwang Juang. *Fundamentals of speech recognition*. Prentice Hall Signal Processing series. Prentice Hall, 1993.

13 Günter Rote. Lexicographic fréechet matchings. In *Proceedings of the 32st European Workshop on Computational Geometry*, pages 101–104, 2014.